

Neutral current (e^-p) cross sections at high Bjorken- x

Ronen Ingbir* †

on behalf of the ZEUS Collaboration

Tel-Aviv University

E-mail: ronen@alzt.tau.ac.il

The Neutral Current (NC) e^-p cross section at high Q^2 and high Bjorken- x values was measured using 187 pb^{-1} of data collected with the ZEUS detector at the HERA accelerator. The analysis relies on the presence of jets expected in high Q^2 events and a new method is proposed to reconstruct the kinematic variable x with improved resolution. The measurement will provide an additional constraint on existing parton density functions (PDFs) of the proton.

XVIII International Workshop on Deep-Inelastic Scattering and Related Subjects, DIS 2010

April 19-23, 2010

Firenze, Italy

*Speaker.

†Supported by the Israel Science Foundation (ISF)

1. Introduction and motivation

The knowledge of the proton structure is mostly derived from deep inelastic scattering (DIS), which is by far the most accurate process for extracting parton density function of the proton (PDFs) ([1]). These PDFs cannot be calculated from first principles and need to be extracted from measurements. A precise knowledge of PDFs in the full kinematic range is particularly important now that the Large Hadron Collider (LHC) has started to deliver the first proton-proton collisions. In DIS, a lepton interacts with a proton by the exchange of a gauge vector boson, which couples to the quarks in the proton and the reaction can be treated as an incoherent sum over all quarks in the proton. In QCD, the parton distributions depend on Q^2 , the virtuality of the exchange boson, and this dependence is described by the QCD evolution equations - the DGLAP equations [2]. The DGLAP evolution equations consist of a set of two coupled differential equations, which can predict the value of parton distributions at any given Q^2 and x_0 , where x is the fraction of the proton momentum carried by the parton, provided all parton distributions are known for all $x > x_0$ at some initial value of $Q_0^2 < Q^2$. A closer look at the existing data for a proton target shows that the only measurements that exist for $x > 0.7$ are either from SLAC (low Q^2) [3] or BCDMS [4] ($Q^2 < 200 \text{ GeV}^2$), where in the latter case the highest achieved x is at 0.75. These high x data points can only be accommodated in the global fits by the inclusion of ad-hoc higher twist effects ([5]). Even so, data for $x > 0.9$ are a factor two higher than the parametrization [6]. A first attempt to explore the region of $x \approx 1$ and $Q^2 > 200 \text{ GeV}^2$ was performed by the ZEUS collaboration on the 96-00 data [7]. In that measurement, at the highest x , the Standard Model predictions (CTEQ6D) tend to slightly underestimate the data. The purpose of these measurements is to confront the understanding of the proton structure at high- x , to possibly establish the region of dominance of the leading twist in the proton structure function and to provide a reliable understanding of the proton structure in the valence region. The measurement presented here was performed with the data collected with the ZEUS detector after the luminosity upgrade of the HERA accelerator (HERA II) using new techniques. During that period, HERA was colliding 920 GeV protons with longitudinally polarized electrons and positrons of 27.5 GeV. Also the ZEUS detector was upgraded with forward tracking [8] and a microvertex detector [9], both of which are important in reducing systematic uncertainties in the measurements of high- x cross sections, especially at high Q^2 .

2. Methodology

A typical high- x and high- Q^2 event in NC DIS consists of the scattered electron and a high energy collimated jet of particles following the direction of the scattered quark. The proton remnants mostly disappear down the beam pipe.

These events are easy to trigger on. The typical property is the presence of a scattered electron and a high value of the variable δ , $\delta = \sum_i E_i - p_{Z_i}$, where the sum is over all the particles and $E_i(p_{Z_i})$ is the energy (Z-component of the momentum, where the Z-axis is defined along the initial proton momentum-vector) of the i -th particle. A requirement of a high value for the measured δ ensures a pure sample of DIS events. Note that the loss of particles along the proton remnant direction does not affect the value of δ . Further selection is based on reconstructed events. The kinematic range accessible to the measurement is determined by the resolution on x and Q^2 . There are various

methods to calculate x and Q^2 ([10]). In high- x events, the electron detection efficiency is close to 100%. The measured four-momentum vector of the scattered electron (electron-method) provides a good resolution on the determination of the momentum transfer squared Q^2 ,

$$Q_e^2 = 2E_e E_e' (1 + \cos\theta), \quad (2.1)$$

where Q_e^2 denotes the Q^2 estimator obtained from the electron variables, E_e is the initial energy of the electron and E_e' and θ (measured with respect to the proton direction) are the energy and the polar angle of the scattered electron, respectively. High- x correlates to low inelasticity, y , and for a given value of Q^2 its error propagates like $\Delta x \approx \frac{\Delta y}{y^2}$. As a result, the resolution on x is poor for $x > 0.1$ and there is no distinction between large and medium x values. In order to improve the x measurement in the ZEUS detector, information on the hadronic final state can be included. For very high x , the struck quark carries a large fraction of the proton energy and the corresponding hadronic system is boosted along the proton direction forming a collimated jet. This topological property may be used to improve the reconstruction of x (jet method). In the analysis, the k_T algorithm [11] in the massless mode is used to find jets in the final state and the jet variables are defined according to the Snowmass convention [12]. The jet information can then be used to calculate x ,

$$x = \frac{E_{\text{jet}}(1 + \cos\theta_{\text{jet}})}{2E_p \left(1 - \frac{E_{\text{jet}}(1 - \cos\theta_{\text{jet}})}{2E_e}\right)}, \quad (2.2)$$

where E_p is the proton beam energy, E_{jet} is the jet energy and θ_{jet} is the jet polar angle. At high- x , θ_{jet} is small and $x \approx E_{\text{jet}}/E_p$. The advantage of the jet method is its low sensitivity to the initial state electromagnetic radiation and a good x resolution. In order to get an unbiased estimate of the jet energy and angle, the jet has to be fully contained in the detector. This imposes a limit on the minimal jet angle. For a fixed Q^2 , the minimum value of y which can be measured determines the highest x value (x_{max}) that can be estimated using this method. For events with only an electron present in the detector, the integrated cross section can be measured. This approach was recently implemented by ZEUS on the HERA-I data [7]. Since the momentum and energy of the electron are measured more precisely than the jet energy, in the present analysis a new approach was implemented in which the jet energy term in eq. (2.2) was determined from the electron measurement assuming p_T balance,

$$E_{\text{jet}} = p_{T\text{jet}}/\sin\theta_{\text{jet}} = p_{Te}/\sin\theta_{\text{jet}}. \quad (2.3)$$

This leads to

$$x = \frac{p_{Te}/\sin\theta_{\text{jet}}(1 + \cos\theta_{\text{jet}})}{2E_p \left(1 - \frac{p_{Te}/\sin\theta_{\text{jet}}(1 - \cos\theta_{\text{jet}})}{2E_e}\right)}. \quad (2.4)$$

Using this method for one-jet events resulted in a 25% improved x resolution (for the x reconstruction of multi-jet events we used an expanded version of the jet method).

The method to determine x and Q^2 , with best resolution, depends crucially on the proper energy calibration of the detector. First the electron energy was calibrated in the Barrel Calorimeter (BCAL) using the double angle method prediction and kinematic peak events. NC events with one jet were selected to calibrate the hadronic energy in BCAL and Forward Calorimeter (FCAL) using the transverse momentum balance between the jet and the electron. The hadronic energy scale

enters in the determination of the jet angle, which is a weighted average over possibly different parts of the calorimeter. Using a similar principle, calibrated jets in the BCAL and FCAL were used to calibrate electrons in the FCAL.

3. Results

The analysis was performed on an e^-p data sample corresponding to an integrated luminosity of 187 pb^{-1} . A good agreement between data and MC distributions is achieved in the electron and jet variables. Good agreement between data and MC is also observed in the distributions of Q^2 and x for events with jets and without jets (only Q^2 available for the latter) as presented in Fig. 1.

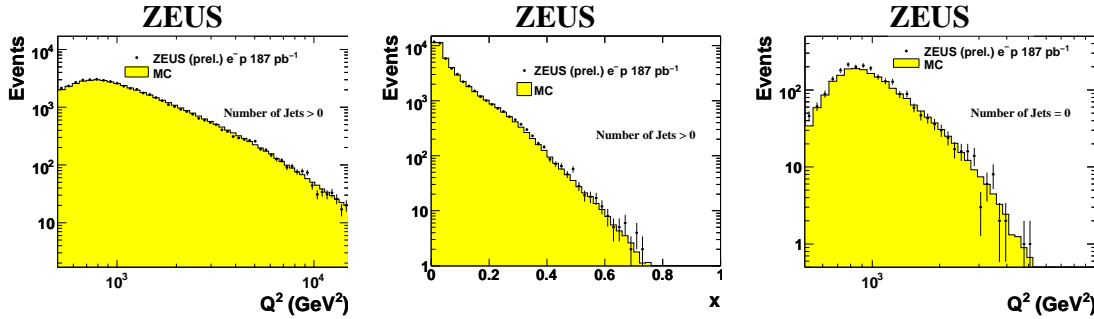


Figure 1: Comparison between e^-p data (points) and MC simulation (histograms) for the distributions of Q^2 (left), x (center), and Q^2 for events without jets (right).

NC DIS cross sections were measured at large values of x including the region $x \approx 1$, in particular for $Q^2 > 400 \text{ GeV}^2$ and $0.1 < x < 1$. Good agreement with Standard Model CTEQ6D predictions is presented for the double differential cross section in Fig. 2. The agreement is good also in the last integrated x bins.

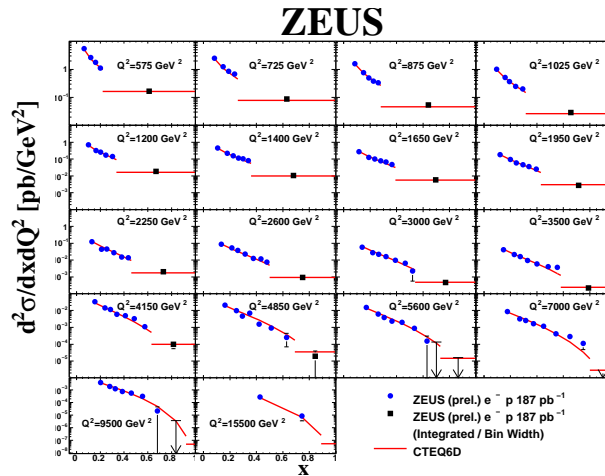


Figure 2: The double differential cross section for e^-p NC scattering at $\sqrt{s} = 318 \text{ GeV}$ (blue circles) and the integral of the double differential cross section divided by the bin width (solid squares) compared to the Standard Model expectations evaluated using CTEQ6D PDFs (red line).

The ratio of the NC cross section to the Standard Model calculations with CTEQ6D are compared to previous ZEUS results (96-97 data with integrated luminosity of 16.7pb^{-1}) and shown in Fig. 3. One of the strong starting points of this analysis is the ability to use the full statistical power of HERA II (much bigger than HERA I) and the inclusion of multi-jet events which reduces systematic uncertainties on the data selection. The improved statistics, better detector understanding and high resolution reconstruction method lead to a higher precision in each bin and to sensitivity to new x bins, higher than ever measured before.

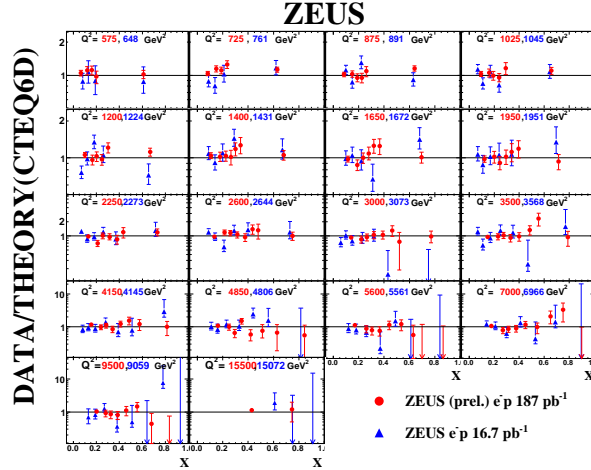


Figure 3: Ratio of the double differential NC e^-p cross section (red circles) and for the 1996-1997 e^-p (blue triangles) to the Standard Model expectation evaluated using the CTEQ6D PDFs.

This measurement is expected to constitute an important constraint not only on PDFs at large x but in the whole phase space, because of the inherent couplings between the small and the large x PDFs.

References

- [1] A. M. Cooper-Sarkar *et al.*, Int. J. Mod. Phys. **A 13**, 3385, (1998)
- [2] Yu. Dokshitzer, Sov. Phys. JETP **46**, 641, (1977); L.N. Lipatov, Sov. J. Nucl. Phys. **20**, 94, (1975);
- [3] P.E. Bosted *et al.*, Phys. Rev. **D 49**, 3091, (1994).
- [4] BCDMS Coll., A.C. Benvenuti *et al.*, Phys. Lett. **B 223**, 485, (1989).
- [5] M. Virchaux and A. Milsztajn, Phys. Lett. **B 274**, 221, (1992).
- [6] S. Rock and P. Bosted, *High Q^2 HERA events and $pQCD$ at high x* , hep-ph/9706436.
- [7] ZEUS Coll., S. Chekanov *et al.*, Eur. Phys. J. **C 49**, 523, (2007)
- [8] ZEUS STT collaboration, S. Fourletov, Nucl. Instrum. Meth. **A 535**, 191, (2004).
- [9] ZEUS collaboration, A. Polini *et al.*, Nucl. Instrum. Meth. **A 581**, 656, (2007)
- [10] U. Bassler and G. Bernardi, Nucl. Instrum. Meth. **A 361**, 197, (1995)
- [11] S. Catani *et al.*, Nucl. Phys. Rev. **D 48**, 3160, (1993).
- [12] E.L Berger, World Scientific 134, (1992).